

Synthesis and Study of Bidentate Benzimidazolylidene–Group 10 Metal Complexes and Related Main-Chain Organometallic Polymers

Andrew J. Boydston, Jonathan D. Rice,[†] Matthew D. Sanderson, Olga L. Dykhno,[†] and Christopher W. Bielawski*

Department of Chemistry and Biochemistry, The University of Texas at Austin, Austin, Texas 78712

Received June 5, 2006

A series of group 10 bis(benzimidazolylidene) complexes featuring chelating N-(*o*-phenol) moieties were synthesized and characterized. The ligand was prepared in 85% overall yield from 1-fluoro-2-nitrobenzene using a short S_NAr/reductive cyclization/alkylation reaction sequence. Direct metalation of the respective benzimidazolium precursor with Ni(II), Pd(II), and Pt(II) salts under ambient atmosphere at 50–80 °C provided the discrete chelating complexes in excellent yields (≥91%). Whereas chelation occurred spontaneously in the case of the Ni complex, an intermediate displaying ligation from the NHCs without chelation from pendent phenol groups was isolated and characterized when Pd was used. This complex was subsequently converted to its chelated form upon treatment with base. The effect of chelation was measured via thermogravimetric analysis and found to enhance the stability of the complex by 24 °C. The chelation also did not significantly effect overall electronic characteristics. A similar reaction sequence was observed when Pt was used, but the respective intermediate could not be isolated. Chelated Ni, Pd, and Pt complexes were characterized by X-ray crystallography and found to exhibit cis configurations about their respective square-planar metal centers. Based on these model systems, a new class of main-chain organometallic polymers comprised of a benzobis(imidazolylidene) ligand with chelating phenolate moieties and group 10 transition metals was synthesized and characterized. The respective bis(bidentate) ligand was prepared from 1,5-dichloro-2,4-dinitrobenzene in three chromatography-free steps in 78% overall yield from commercially-available starting materials and used as monomer. Consistent with the model studies, direct metalation of the monomer was accomplished by addition of a stoichiometric amount of metal(II) salt under basic conditions, which resulted in excellent yields (≥95%) of the respective organometallic polymers with molecular weights up to 363,000 g/mol (relative to polystyrene standards). The polymers were found to be exceptionally air- and moisture-stable and displayed thermal stabilities exceeding 350 °C (under nitrogen), as measured by thermogravimetric analysis. Electronic absorption measurements indicated the λ_{max} values of these polymers ranged between 312 and 322 nm, depending on the incorporated transition metal, and were bathochromically shifted by up to 27 nm relative to their corresponding model complexes.

Introduction

Since the synthesis and isolation of the first stable, crystalline N-heterocyclic carbene (NHC) was disclosed¹ by Arduengo in

the early 1990s (1, Figure 1), the development of new functional organometallic complexes has witnessed tremendous growth.^{2,3} During this time, a structurally diverse range of NHCs, and their complexes with various transition metals, have been studied and employed in numerous synthetic reactions.⁴ The electronic

* Corresponding author. E-mail: bielawski@cm.utexas.edu.

[†] Denotes an undergraduate contributor.

(1) (a) Arduengo, A. J., III; Harlow, R. L.; Kline, M. *J. Am. Chem. Soc.* **1991**, *113*, 361. (b) Arduengo, A. J., III. *Acc. Chem. Res.* **1999**, *32*, 913.

(2) (a) Viciu, M. S.; Nolan, S. P. *Top. Organomet. Chem.* **2005**, *14*, 241.

(b) Scott, N. M.; Nolan, S. P. *Eur. J. Inorg. Chem.* **2005**, 1815. (c) Cavallo,

L.; Correa, A.; Costabile, C.; Jacobsen, H. *J. Organomet. Chem.* **2005**, *690*,

5407. (d) Basato, M.; Michelin, R. A.; Mozzon, M.; Sgarbossa, P.; Tassan,

A. *J. Organomet. Chem.* **2005**, *690*, 5414. (e) Braband, H.; Kückmann, T.

I.; Abram, U. *J. Organomet. Chem.* **2005**, *690*, 5421. (f) Crabtree, R. H. *J.*

Organomet. Chem. **2005**, *690*, 5451. (g) Lappert, M. F. *J. Organomet. Chem.*

2005, *690*, 5467. (h) Frenking, G.; Solá, M.; Vyboishchikov, S. F. *J.*

Organomet. Chem. **2005**, *690*, 6178. (i) Crudden, C. M.; Allen, D. P. *Coord.*

Chem. Rev. **2004**, *248*, 2247. (j) Kavel, K. J.; McGuinness, D. S. *Coord.*

Chem. Rev. **2004**, *248*, 671. (k) Peris, E.; Crabtree, R. H. *Coord. Chem.*

Rev. **2004**, *248*, 2239. (l) César, V.; Bellemin-Laponnaz, S.; Gade, L. H.

Chem. Soc. Rev. **2004**, *33*, 619. (m) Perry, M. C.; Burgess, K. *Tetrahe-*

dron: Asymmetry **2003**, *14*, 951. (n) Herrmann, W. A. *Angew. Chem., Int.*

Ed. **2002**, *41*, 1290. (o) Arnold, P. *Heteroat. Chem.* **2002**, *13*, 534. (p)

Cowley, A. H. *J. Organomet. Chem.* **2001**, *617*–618, 105. (q) Raubenhe-

imer, H. G.; Cronje, S. *J. Organomet. Chem.* **2001**, *617*–618, 170. (r)

Weskamp, T.; Böhm, V. P. W.; Herrmann, W. A. *J. Organomet. Chem.*

2000, *600*, 12. (s) Herrmann, W. A.; Köcher, C. *Angew. Chem., Int. Ed.*

Engl. **1997**, *36*, 2162.

(3) For an example of transition metal–NHC complexes prepared from enetetraamines (NHC dimers), see: Lappert, M. F. *J. Organomet. Chem.* **1988**, *358*, 185.

(4) For recent reviews, see: (a) Hahn, F. E. *Angew. Chem., Int. Ed.* **2006**,

45, 1348. (b) Zeitler, K. *Angew. Chem., Int. Ed.* **2005**, *44*, 7506. (c) Nair,

V.; Bindu, S.; Sreekumar, Y. *Angew. Chem., Int. Ed.* **2005**, *44*, 1907. (d)

Enders, D.; Balensiefer, T. *Acc. Chem. Res.* **2004**, *37*, 534. (e) Bourissou,

D.; Guerret, O.; Gabbai, F. P.; Bertrand, G. *Chem. Rev.* **2000**, *100*, 39.

(5) Pause, L.; Robert, M.; Heinicke, J.; Kühl, O. *J. Chem. Soc., Perkin*

Trans. 2 **2001**, 1383.

(6) For additional syntheses of benzimidazolium and benzimidazolylidene

compounds, see: (a) Huynh, H. V.; Holtgrewe, C.; Pape, T.; Koh, L. L.;

Hahn, F. E. *Organometallics* **2006**, *25*, 245. (b) Hahn, F. E.; Langenhahn,

V.; Lügger, T.; Pape, T.; Le, Van, D. *Angew. Chem., Int. Ed.* **2005**, *44*,

3759. (c) Rivas, F. M.; Riaz, U.; Giessert, A.; Smulik, J. A.; Diver, S. T.

Org. Lett. **2001**, *3*, 2673. (d) Hahn, F. E.; Wittenbecher, L.; Le, Van, D.;

Fröhlich, R. *Angew. Chem., Int. Ed.* **2000**, *39*, 541. (e) Korotkikh, N. I.;

Rayenko, G. F.; Kiselyov, A. V.; Knishevitsky, A. V.; Shvaika, O. P.;

Cowley, A. H.; Jones, J. N.; Macdonald, C. L. B. Synthesis of Stable

Heteroaromatic Carbenes of the Benzimidazole and 1,2,4-Triazole Series

and their Precursors. In *Selected Methods for Synthesis and Modification*

of Heterocycles; Kartsev, V. G., Ed., Moscow, 2002; Vol. 1.

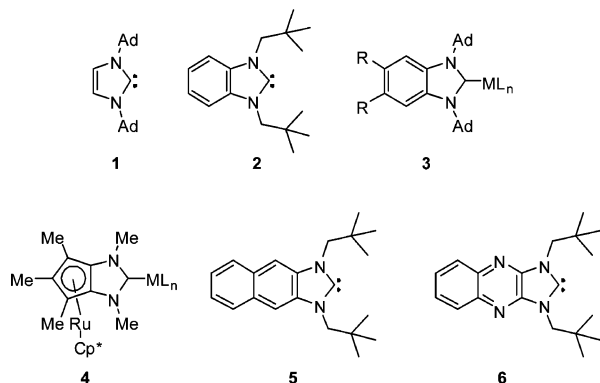


Figure 1. Representative examples of NHCs and NHC–metal complexes.

nature of NHC systems is important in both synthetic and materials chemistry, and quantum chemical studies have shown that annulation significantly impacts this aspect of NHCs.⁵ Experimentally, key advances with annulated NHCs have been made in the areas of benzimidazolylidenes⁶ (e.g., **2**⁷ and **3**⁸), fused metallocenes (e.g., **4**⁹), extended annulated systems (e.g., **5**¹⁰), and heterocycle-fused¹¹ NHCs (e.g., **6**¹²). Collectively, these compounds exhibit remarkable structural tunability and broad metal compatibility, which often results in considerable performance enhancement in their respective metal-catalyzed reactions. Prime examples of such effects have been observed in Pd-mediated carbon–carbon and carbon–heteroatom bond forming reactions and in Ru-mediated olefin metathesis reactions.¹³

In contrast, relatively little attention has been directed toward using NHCs as a means to construct organometallic polymeric materials.¹⁴ Considering the large amount of synthetic and functional diversity inherent to NHCs coupled with their high affinity toward a wide range of transition metals, they are ideally suited for this purpose. However, to obtain polymeric materials, access to multitopic NHCs capable of binding at least two transition metals with high fidelity is essential.¹⁵ Although many

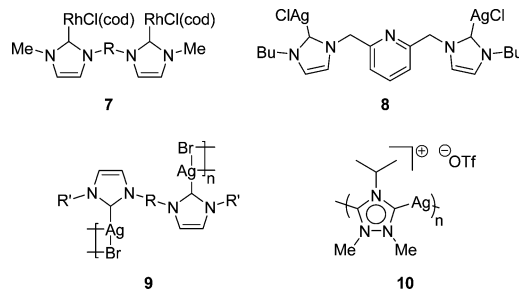


Figure 2. Representative examples of NHC-based bimetallic complexes and related solid-state polymers.

di-, tri-, and multitopic NHC-based ligands are known,^{20,16} they are often poised (and designed) to preferentially bind to one metal center in a chelating or pincer-type fashion. Notable exceptions (Figure 2) include systems from Herrmann (**7**),¹⁷ Youngs (**8**),¹⁸ and Lee (**9**),¹⁹ who have each shown that some pincer-type bis(carbene)s form bimetallic structures (with 1:1 NHC/metal stoichiometry). In particular, with Ag(I) salts, materials could be obtained that were polymeric in the solid-state. However, dissolution of these materials affords the respective discrete bimetallic complexes.¹⁹ In a related example, Bertrand²⁰ reported that non-chelating bis(carbene)s based on trialkylated 1,2,4-triazoles (**10**) also afforded solid-state polymers with Ag(I) salts.²¹ These results suggested that tuning the NHC–metal interaction in corresponding organometallic polymers may ultimately lead to new advances in electronic materials¹⁴ or in responsive materials, analogous to those of Craig²² and Rowan.²³

We have recently launched a program focused on utilizing multitopic NHCs as the key constituents in producing soluble, processable, and high molecular weight materials, particularly those with tunable electronic properties and responsive characteristics.²⁴ We have shown that various linearly opposed bis(imidazolium) salts (**11**) can be easily prepared and function as effective precursors to NHC-based organometallic materials.^{24,25} Specifically, as shown in Scheme 1, they can be copolymerized with transition metals to form high molecular weight main-chain

(7) Hahn, F. E.; Wittenbecher, L.; Boese, R.; Bläser, D. *Chem. Eur. J.* **1999**, *5*, 1931.

(8) (a) Hadei, N.; Kantchev, E. A. B.; O'Brien, C. J.; Organ, M. G. *Org. Lett.* **2005**, *7*, 1991. (b) O'Brien, C. J.; Kantchev, E. A. B.; Chass, G. A.; Hadei, N.; Hopkinson, A. C.; Organ, M. G.; Setiadi, D. H.; Tang, T.-H.; Fang, D.-C. *Tetrahedron* **2005**, *61*, 9723.

(9) Arduengo, A. J., III; Tapu, D.; Marshall, W. J. *J. Am. Chem. Soc.* **2005**, *127*, 16400.

(10) Saravanakumar, S.; Oprea, A. I.; Kindermann, M. K.; Jones, P. G.; Heinicke, J. *Chem. Eur. J.* **2006**, *12*, 3143.

(11) For purine-based annulated NHCs, see: (a) Schütz, J.; Herrmann, W. A. *J. Organomet. Chem.* **2004**, *689*, 2995. (b) Kascatan-Nebioglu, A.; Panzner, M. J.; Garrison, J. C.; Tessier, C. A.; Youngs, W. J. *Organometallics* **2004**, *23*, 1928.

(12) Saravanakumar, S.; Kindermann, M. K.; Heinicke, J.; Köckerling, M. *Chem. Commun.* **2006**, 640.

(13) For recent reviews, see: (a) Christmann, U.; Vilar, R. *Angew. Chem., Int. Ed.* **2005**, *44*, 366. (b) Hillier, A. C.; Grasa, G. A.; Viciu, M. S.; Lee, H. M.; Yang, C.; Nolan, S. P. *J. Organomet. Chem.* **2002**, *653*, 69. (c) Trnka, T. M.; Grubbs, R. H. *Acc. Chem. Res.* **2001**, *34*, 18.

(14) For general reviews on organometallic polymers, see: (a) Swager, T. M. in *Progress in Inorganic Chemistry*; Karlin, K. D., Ed.; Wiley-VCH: 1999; Vol. 48. (b) Pittman, C. U. *J. Inorg. Organomet. Polym. Mater.* **2005**, *15*, 33. (c) Moorlag, C.; Sih, B. C.; Stott, T. L.; Wolf, M. O. *J. Mater. Chem.* **2005**, *15*, 2433. (d) Gianneschi, N. C.; Masar, M. S., III; Mirkin, C. A. *Acc. Chem. Res.* **2005**, *38*, 825. (e) Bunz, U. H. F. *J. Organomet. Chem.* **2003**, *683*, 269. (f) Nguyen, P.; Gómez-Elipé, P.; Manners, I. *Chem. Rev.* **1999**, *99*, 1515. (g) Roncali, J. *J. Mater. Chem.* **1999**, *9*, 1875. (h) Pickup, P. G. *J. Mater. Chem.* **1999**, *9*, 1641. For a tutorial review on main-chain organometallic polymers, see: Williams, K. A.; Boydston, A. J.; Bielawski, C. W. *Chem. Soc. Rev.* **2006**, in press (DOI: 10.1039/b601574n).

(15) Boydston, A. J.; Bielawski, C. W. *Dalton Trans.* **2006**, 4073.

(16) (a) Gehrhus, B.; Hitchcock, P. B.; Lappert, M. F. *Z. Anorg. Allg. Chem.* **2005**, *631*, 1383. (b) Hu, X.; Meyer, K. *J. Organomet. Chem.* **2005**, *690*, 5474. (c) Clyne, D. S.; Jin, J.; Genest, E.; Gallucci, J. C.; RajanBabu, T. V. *Org. Lett.* **2000**, *2*, 1125. (d) Herrmann, W. A.; Schwarz, J.; Gardiner, M. G. *Organometallics* **1999**, *18*, 4082. (e) Herrmann, W. A.; Köcher, C.; Gooßen, L. J.; Artus, G. R. *J. Chem. Eur. J.* **1996**, *2*, 1627. (f) Herrmann, W. A.; Reisinger, C.-P.; Spiegler, M. *J. Organomet. Chem.* **1998**, *557*, 93. (g) Fehllhammer, W. P.; Bliss, T.; Kernbach, U.; Brüdgam, I. *J. Organomet. Chem.* **1995**, *490*, 149.

(17) Herrmann, W. A.; Elison, M.; Fischer, J.; Köcher, C.; Artus, G. R. *J. Chem. Eur. J.* **1996**, *2*, 772.

(18) Simons, R. S.; Custer, P.; Tessier, C. A.; Youngs, W. J. *Organometallics* **2003**, *22*, 1979.

(19) Chiu, P. L.; Chen, C. Y.; Zeng, J. Y.; Lu, C. H.; Lee, H. M. *J. Organomet. Chem.* **2005**, *690*, 1682.

(20) Guerret, O.; Solé, S.; Gornitzka, H.; Teichert, M.; Trinquier, G.; Bertrand, G. *J. Am. Chem. Soc.* **1997**, *119*, 6668.

(21) A glycouril-based bis(carbene) precursor affords discrete bimetallic complexes when reacted with Ag₂O or Hg(OAc)₂, and insoluble polymers when reacted with Pd(OAc)₂, see: Li, W. Ph.D. Thesis, University of Alabama, Tuscaloosa, 2004.

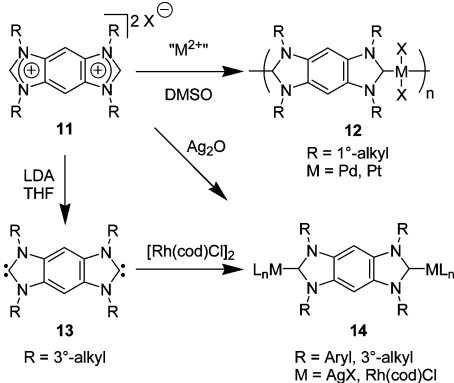
(22) (a) Yount, W. C.; Loveless, D. M.; Craig, S. L. *J. Am. Chem. Soc.* **2005**, *127*, 14488. (b) Yount, W. C.; Juwarker, H.; Craig, S. L. *J. Am. Chem. Soc.* **2003**, *125*, 15302.

(23) Beck, J. B.; Rowan, S. J. *J. Am. Chem. Soc.* **2003**, *125*, 13922. For a related review on responsive materials using dynamic covalent chemistry, see: Rowan, S. J.; Cantrill, S. J.; Cousins, G. R. L.; Sanders, J. K. M.; Stoddart, J. F. *Angew. Chem., Int. Ed.* **2002**, *41*, 898.

(24) Boydston, A. J.; Williams, K. A.; Bielawski, C. W. *J. Am. Chem. Soc.* **2005**, *127*, 12496.

(25) (a) Boydston, A. J.; Khravov, D. M.; Bielawski, C. W. *Tetrahedron Lett.* **2006**, *47*, 5123. (b) Khravov, D. M.; Boydston, A. J.; Bielawski, C. W. *Org. Lett.* **2006**, *8*, 1831.

Scheme 1. Current Synthetic Applications of Annulated Bis(NHC)s



organometallic polymers that retain their structure in solution (e.g., **12**),²⁴ deprotonated to generate “Janus-type” free bis(carbene)s **13**, or metallated to give discrete (monomeric) bimetallic systems **14**.²⁶ One limitation of our initial approach to metal-containing polymers was that the range of compatible transition metals was confined to Pd(II) and Pt(II) salts. Use of other metals (e.g., Ni) resulted in labile polymeric materials that rapidly underwent solvolysis in the presence of protic media (e.g., H₂O and MeOH). To increase control over material, physical, and electronic properties, we desired a method for overcoming this constraint and expanding the scope of compliant transition metals in NHC-based organometallic polymers. This required the design and synthesis of a new ditopic NHC-based monomer that was appropriately functionalized to exhibit enhanced affinities toward transition metals. In addition, we sought a design that was flexible and would not compromise the ability to independently tune other characteristics of the resulting polymeric materials (solubilities, electronics, etc.).

An exemplary strategy for enhancing the chemical stability of metal–NHC interactions is to incorporate a bidentate, or chelating, scaffold into the NHC architecture. For example, enhanced stability of a Cu–NHC complex was demonstrated in Hoveyda’s²⁷ use of imidazolylidene ligands containing N-aryloxy units. Similarly, Grubbs²⁸ utilized N-(2-hydroxyphenyl)-substituted imidazolium salts to complex to Pd(II) species in a chelating-type fashion. While many other examples of mixed multidentate carbene ligands built on various types of imidazole-based frameworks are known,²⁹ related bidentate benzimidazolylidenes have received considerably less attention. Key examples are depicted in Figure 3 and include Ir-based

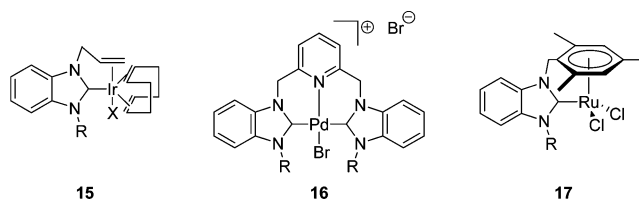


Figure 3. Representative examples of chelating benzimidazolylidene–metal complexes.

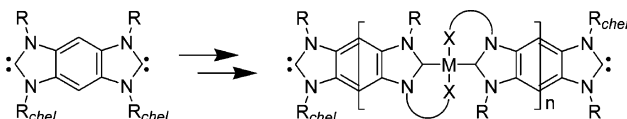


Figure 4. Generalized depiction of a ditopic NHC displaying a single chelating N substituent (R_{chel}) on each carbene “face.”

complexes using chelating olefinic groups (**15**),³⁰ Pd-pincer complexes comprised of a difunctional pyridine bridge (**16**),³¹ and a Ru-containing complex that exhibits intramolecular chelation through metallocene formation (**17**).³² For the purpose of forming macromolecular materials suitable for use in electronic applications, benzannulated systems are particularly attractive since the arene linkers maintain formal conjugation within the corresponding main chains of the polymeric materials and should permit electronic tuning through further derivatization.³³ However, incorporation of chelating groups into multi-topic, annulated frameworks designed for macromolecular applications presents specific synthetic challenges.

Installation of the appropriate (i.e., chelating) N-substituents in a regiospecific manner about a benzobis(imidazole) system (e.g., **11**), for example, can be nontrivial. Aryl amination, a method that has been successfully used for the synthesis of benzimidazolium compounds,^{6c} is reluctant to give high yields of regioselective amination products when tetrahalobenzenes are used.^{25b} Likewise, regioselective alkylation of benzobis(imidazole) would be expected to be challenged by similar difficulties. Furthermore, formation of main-chain polymers with transition metals that prefer four-coordinate geometries, e.g., Ni(II), requires a ditopic NHC ligand where each carbene “face” of the monomer is desymmetrized³⁴ to contain only one chelating N-substituent (Figure 4). Ultimately, a new synthetic route to prepare such ditopic bis(bidentate) NHC systems was needed.

Synthetic methods used to prepare NHC–metal complexes typically utilize one of three strategies: (1) reaction of an azolium salt with an electrophilic metal species possessing basic counterions or coordinating anions,^{16d,35} (2) generation of the free carbene followed by introduction of an electrophilic metal species,^{2–4} or (3) formation of a Ag(I)–NHC complex followed by ligand transfer to the desired transition metal.³⁶ While each of the aforementioned methods are excellent for constructing small-molecule systems, none seemed directly amenable to

(26) Khranov, D. M.; Boydson, A. J.; Bielawski, C. W. *Angew. Chem., Int. Ed.* **2006**, *45*, 6186.

(27) (a) Veldhuizen, J. J. V.; Campbell, J. E.; Giudici, R. E.; Hoveyda, A. H. *J. Am. Chem. Soc.* **2005**, *127*, 6877. (b) Larsen, A. O.; Leu, W.; Oberhuber, C. N.; Campbell, J. E.; Hoveyda, A. H. *J. Am. Chem. Soc.* **2004**, *126*, 11130.

(28) Waltmann, A. W.; Grubbs, R. H. *Organometallics* **2004**, *23*, 3105.

(29) For selected examples, see: (a) Inamoto, K.; Kuroda, J.-I.; Hiroya, K.; Noda, Y.; Watanabe, M.; Sakamoto, T. *Organometallics* **2006**, *25*, 3095. (b) Legault, C. Y.; Kendall, C.; Charette, A. B. *Chem. Commun.* **2005**, 3826. (c) Clavier, H.; Coutable, L.; Toupet, L.; Guillemin, J.-C.; Mauduit, M. *J. Organomet. Chem.* **2005**, *690*, 5237. (d) Jensen, T. R.; Schaller, C. P.; Hillmyer, M. A.; Tolman, W. B. *J. Organomet. Chem.* **2005**, *690*, 5881. (e) Li, W.-F.; Sun, H.-M.; Wang, Z.-G.; Chen, M.-Z.; Shen, Q.; Zhang, Y. *J. Organomet. Chem.* **2005**, *690*, 6227. (f) Liddle, S. T.; Arnold, P. L. *Organometallics* **2005**, *24*, 2597. (g) Li, W.; Sun, H.; Chen, M.; Wang, Z.; Hu, D.; Shen, Q.; Zhang, Y. *Organometallics* **2005**, *24*, 5925. (h) Clavier, H.; Coutable, L.; Guillemin, J.-C.; Mauduit, M. *Tetrahedron: Asymmetry* **2005**, *16*, 921. (i) Arnold, P. L.; Scarisbrick, A. C.; Blake, A. J.; Wilson, C. *Chem. Commun.* **2001**, 2340.

(30) Hahn, F. E.; Holtgrewe, C.; Pape, T.; Martin, M.; Sola, E.; Oro, L. A. *Organometallics* **2005**, *24*, 2203.

(31) Hahn, F. E.; Jahnke, M. C.; Gomez-Benitez, V.; Morales-Morales, D.; Pape, T. *Organometallics* **2005**, *24*, 6458.

(32) Çetinkaya, B.; Demir, S.; Özdemir, I.; Toupet, L.; Sémeril, D.; Bruneau, C.; Dixneuf, P. G. *Chem. Eur. J.* **2003**, *9*, 2323.

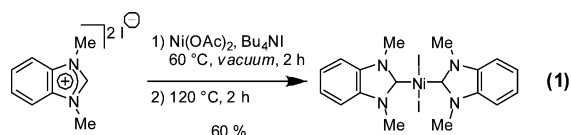
(33) (a) O’Brien, C. J.; Kantchev, E. A. B.; Chass, G. A.; Hadei, N.; Hopkinson, A. C.; Organ, M. G.; Setiadi, D. H.; Tang, T.-H.; Fang, D.-C. *Tetrahedron* **2005**, *61*, 9723. (b) Hadei, N.; Kantchev, E. A. B.; O’Brien, C. J.; Organ, M. G. *Org. Lett.* **2005**, *7*, 1991.

(34) In this context, the term “desymmetrized” refers to a system in which each imidazole moiety features two different N-substituents.

(35) Tulloch, A. A. D.; Danopolous, A. A.; Kleinhenze, S.; Light, M. E.; Hursthouse, M. B.; Eastham, G. *Organometallics* **2001**, *20*, 2027.

(36) Wang, H. M. J.; Lin, I. J. B. *Organometallics* **1998**, *17*, 972.

forming stable, high molecular weight polymers with metals other than Pd and Pt. Examples of specific challenges can be found by surveying known Ni–NHC complexes. For example, Herrmann demonstrated that imidazolylidene–Ni(II) complexes can be obtained directly from their respective imidazolium salts in 30% yield using Ni(OAc)₂.³⁷ While this was an outstanding synthetic achievement, this yield is too low for forming high polymer and the reaction must be conducted in the melt under vacuum using anhydrous reagents. Synthesis of benzimidazolylidene-based Ni complexes using this methodology was found to be challenged by the fact that the resulting complexes decompose at the high reaction temperatures required (150 °C).³⁸ However, Hahn accomplished the first synthesis of benzimidazolylidene–Ni(II) complexes³⁸ using an elegant adaptation of Herrmann's procedure. By combining benzimidazolium salts with tetrabutylammonium salts at elevated temperatures under vacuum (eq 1), the ammonium salts were melted to give an ionic liquid solvent system. This ultimately allowed for reduced reaction temperatures (120 °C) and afforded the desired Ni complexes in 28–60% yield. Since reaction yields of >95% are typically necessary to obtain high molecular weight polymer,³⁹ and mild polymerization reaction conditions are desirable, the development of a new, universal protocol for forming benzimidazolylidene–transition metal complexes was targeted.



Considering alternatives to direct metalation of azolium salts, free carbene generation is compatible with essentially all transition metals known to form complexes with NHCs. Caveats of this approach, however, include a two-step procedure under an inert atmosphere and the use of dry solvents to avoid destruction of the free carbene. When carbene dimerization can occur, the resulting enetetraamines^{6d,40} are extremely sensitive toward oxygen and often subject to rearrangement or fragmentation, depending on the nature of the N-substituent.⁴¹ Although benzobis(imidazolylidene)s can be manipulated as either their free carbenes^{25b} or respective homopolymers⁴² en route to bimetallics and metallopolymers, this imposes limitations on

(37) Herrmann, W. A.; Gerstberger, G.; Spiegler, M. *Organometallics* **1997**, *16*, 2009.

(38) Huynh, H. V.; Holtgrewe, C.; Pape, T.; Koh, L. L.; Hahn, F. E. *Organometallics* **2006**, *25*, 245.

(39) (a) Odian, G. *Principles of Polymerization*; Wiley: Hoboken, NJ, 2004; pp 39–63. (b) Carothers, W. H. *Trans. Faraday Soc.* **1936**, *32*, 39.

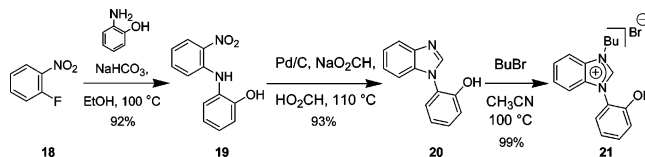
(40) (a) Shi, Z.; Thummel, R. P. *J. Org. Chem.* **1995**, *60*, 5935. (b) Winberg, H. E.; Downing, J. R.; Coffman, D. D. *J. Am. Chem. Soc.* **1965**, *87*, 2054.

(41) Çetinkaya, B.; Çetinkaya, E.; Chamizo, J. A.; Hitchcock, P. B.; Jasim, H. A.; Küçükbay, H.; Lappert, M. F. *J. Chem. Soc., Perkin Trans. I* **1998**, 2047.

(42) Kamplain, J. W.; Bielawski, C. W. *Chem. Commun.* **2006**, 1727.

(43) For an excellent review on Ag–NHC complexes, see: Garrison, J. C.; Youngs, W. J. *Chem. Rev.* **2005**, *105*, 3978. For other examples demonstrating carbene transfer from related Ag complexes, see: (a) de Frémont, P.; Scott, N. M.; Stevens, E. D.; Nolan, S. P. *Organometallics* **2005**, *24*, 2411. (b) Veldhuizen, J. J. V.; Campbell, J. E.; Giudici, R. E.; Hoveyda, A. H. *J. Am. Chem. Soc.* **2005**, *127*, 6877. (c) Arnold, P.; Searisbrick, A. C. *Organometallics* **2004**, *23*, 2519. (d) Catalano, V. J.; Malwitz, M. A.; Etogo, A. O. *Inorg. Chem.* **2004**, *43*, 5714. (e) Larsen, A. O.; Leu, W.; Oberhuber, C. N.; Campbell, J. E.; Hoveyda, A. H. *J. Am. Chem. Soc.* **2004**, *126*, 11130. (f) Chianese, A. R.; Li, X.; Janzen, M. C.; Faller, J. W.; Crabtree, R. H. *Organometallics* **2003**, *22*, 1663. (g) Simons, R. S.; Custer, P.; Tessier, C. A.; Youngs, W. J. *Organometallics* **2003**, *22*, 1979. (h) Tulloch, A. A. D.; Danopoulos, A. A.; Tizzard, G. J.; Coles, S. J.; Hursthouse, M. B.; Hay-Motherwell, R. S.; Motherwell, W. B. *Chem. Commun.* **2001**, 1270.

Scheme 2. Synthesis of Phenol-Substituted Benzimidazolium Salt 21



compatible solvents. For example, high molecular weight materials are generally precluded by limited solubilities in common organic media (THF, benzene, PhCH₃, etc.). One method that has been employed with a diverse array of conditions, solvents, and substrates is Lin's NHC-transfer method.^{36,43} However, disposal of stoichiometric Ag salts and confirmation of quantitative Ag exchange is not ideal for macromolecular applications.

With these considerations in mind, we targeted a ligand design that alleviated the need for strict use of inert atmospheres and allowed access to stable NHC complexes via direct metalation of benzimidazolium salts in a single step and in high yields. Herein, we report our efforts to expand the range of transition metals that can be incorporated into NHC-based main-chain organometallic polymers via direct metalation of bis(azolium) salts bearing chelating N-(*o*-phenol) moieties. In particular, we aimed to increase the binding affinity within bis(NHC)–metal systems without compromising control over electronic properties. Our initial efforts focused on the synthesis and study of discrete complexes designed to mimic the repeating metal centers in their corresponding main-chain polymers. Building from these results, we turned our attention toward designing and deploying analogous ditopic systems that were prone to polymerize. The results of these investigations follow.

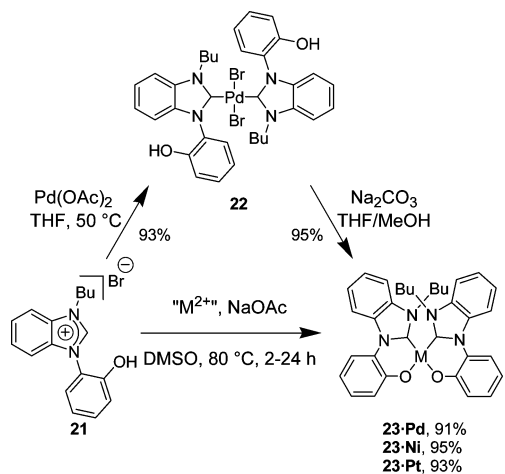
Results and Discussion

Prior to engaging in the synthesis of polymeric materials, we first investigated the propensity of a phenol-substituted benzimidazolium salt to undergo metalation and chelation with group 10 metal(II) species. This would provide insight into the chelation event and allow for characterization of model complexes representative of the repeat units of their respective polymer chains. Thus, a benzimidazolium salt containing a pendent N-(*o*-phenol) group was synthesized as shown in Scheme 2. Aryl amination of 1-fluoro-2-nitrobenzene (**18**) with 2-aminophenol under basic conditions⁴⁴ provided the respective diarylamine **19** in 92% yield.⁴⁵ We envisioned that reduction of the nitro group followed by formylative cyclization of the resulting diamino intermediate could be accomplished using a “one-pot” protocol. This was successfully executed by using a mixture of NaO₂CH/HO₂CH in the presence of catalytic amounts of Pd/C, which effectively hydrogenated the nitro group in situ. Within 1–2 h, the intense red-orange color associated with nitroarene **19** had dissipated, indicating complete reduction had been accomplished. Continued heating (up to 10 h) ultimately provided the formylatively cyclized product **20**, which was obtained after removal of Pd/C via filtration and neutralization of the filtrate with aqueous base.⁴⁶ The crude benzimidazole was collected and alkylated with 1-bromobutane in CH₃CN

(44) For similar S_NAr reactions using 1-fluoro-2-nitrobenzene, see: (a) Shi, M.; Qian, H. *Tetrahedron* **2005**, *61*, 4949. (b) Murahashi, S.-I.; Ono, S.; Imada, Y. *Angew. Chem., Int. Ed.* **2002**, *41*, 2366.

(45) For an alternate synthesis of **19**, see: Allinger, N. L.; Youngdale, G. A. *J. Am. Chem. Soc.* **1962**, *84*, 1020.

(46) For an alternative synthesis of **20**, see: Tashiro, M.; Itoh, T.; Fukata, G. *Synthesis* **1982**, 217.

Scheme 3. Synthesis of Model Complexes 22·Pd and 23 (yields of 23 represent the direct conversion from 21)

followed by removal of volatiles under vacuum to give benzimidazolium bromide **21**.⁴⁷ The overall yield for this reaction sequence was 85%. Due to the N-butyl group, this hygroscopic azolium salt was soluble in polar organic solvents (e.g., CH_2Cl_2 , CHCl_3 , THF, CH_3CN , and DMSO).

With **21** in hand, we were poised to investigate the efficiency of metal complexation. Given that direct metalation of azolium salts with Pd(II) species is a well-established protocol that gives rise to stable metal complexes, we targeted a chelated Pd(II) model system. Benzimidazolium salt **21** was thus treated with 0.5 equiv of Pd(OAc)_2 in THF at 50 °C for 2 h. Analysis of the crude product mixture by ^1H NMR spectroscopy confirmed that no residual azolium species remained (diagnostic azolium ^1H signal: $\delta = 10.8$ ppm in $\text{DMSO-}d_6$). However, the phenol moieties did not appear to be chelated to the metal center, as broad singlets were observed at $\delta = 10.0$ and 9.9 ppm in the ^1H NMR spectrum (solvent = $\text{DMSO-}d_6$) and a strong signal was observed at 3331 cm^{-1} in the IR spectrum of this complex. Mass spectral analysis supported a palladium dibromide species ligated by two NHC ligands consistent with structure **22·Pd** shown in Scheme 3. The methylene units of the butyl groups appeared in the ^1H NMR spectrum as complex multiplets, which, in combination with the observation of two distinct hydroxyl signals, suggested that isomeric structures may be present in solution (e.g., relative syn and anti conformations may exist from possible cis and trans isomers).

To investigate the structure of **22·Pd**, X-ray-quality crystals were obtained as light brown prisms by diffusion of hexanes into a THF solution of the product mixture. The ORTEP diagram shown in Figure 5 confirmed the non-chelated structure of this complex (selected crystal data are summarized in Table 1). The crystallized product existed in a relative trans geometry about the square-planar metal center (C1-Pd-C1^* and C1-Pd-Br bond angles = 180.0° and 88.9° , respectively) with each butyl group experiencing a π -facial interaction with the phenol ring of the complementary NHC ligand (nearest interatomic distance: C11-C16 , 3.97 Å). Most notably, the phenol rings were twisted nearly perpendicular to the plane of the benzimidazolylidene (average dihedral angle = 68°) with essentially no discernible interaction between either phenol oxygen and the Pd atom (average distance = 3.99 Å). The $\text{Pd-C}_{\text{carbene}}$ bond length of 2.02 Å was consistent with other benzimidazolylidene—

Pd(II) complexes, as was the carbene signal found at $\delta = 181$ ppm in the ^{13}C NMR spectrum (solvent = CDCl_3).

Complex **22·Pd** appeared to be stable to air and moisture, and thermogravimetric analysis (TGA) revealed a $T_d = 287^\circ\text{C}$ under an atmosphere of nitrogen. Finally, the complex showed good solubility in most polar organic solvents (e.g., CH_2Cl_2 , CHCl_3 , THF, and MeOH).

To facilitate chelation, crystals of **22·Pd** were redissolved in THF and treated with a methanolic solution of Na_2CO_3 for 1 h under ambient conditions. After aqueous workup, spectroscopic analysis of the product suggested successful chelation and clean formation of complex **23·Pd**. Signals corresponding to hydroxyl groups were not observed in either the ^1H NMR or IR spectrum of this complex. In contrast to **22·Pd**, the ^1H NMR spectrum of **23·Pd** represented a single isomer with a NCH_2 triplet at $\delta = 4.9$ ppm.

To confirm and study the molecular structure of **23·Pd**, X-ray-quality crystals were obtained as yellow laths by slow evaporation of a THF/hexanes solution of the complex. Surprisingly, the X-ray data (represented as an ORTEP diagram in Figure 6)⁴⁹ revealed that the relative geometry about the metal center was now cis.⁵⁰ The metal center remained square-planar as expected with C1-Pd-O1^* and C1-Pd-C1^* bond angles of 173.2° and 99.3° , respectively. The $\text{Pd-C}_{\text{carbene}}$ bond length (1.94 Å) was slightly shorter than those typically observed in benzimidazolylidene—Pd(II) complexes (1.97–2.02 Å), including the $\text{Pd-C}_{\text{carbene}}$ bond length observed for **22·Pd** (2.02 Å).^{10,48} It is important to note, however, that the majority of related benzimidazolylidene—Pd(II) complexes contain Pd—halide bonds, whereas **23·Pd** contains Pd—O bonds; thus, different trans influences may be expected. In addition, chelation effects may also contribute to the relative shortening of the $\text{Pd-C}_{\text{carbene}}$ bond. The N-C-N bond angle (105.6°) and ^{13}C NMR resonance at $\delta = 178$ ppm were consistent with other known benzimidazolylidene—Pd(II) complexes.^{10,48} The slight upfield shift of the carbene signal (relative to **22·Pd**, $\delta = 181$ ppm) may reflect increased electron density at the metal center as a result of the Pd—O bonds. Interestingly, chelation appeared (qualitatively) to impart greater solubility (relative to **22·Pd**) as complex **23·Pd** readily dissolved in common organic solvents such as CH_2Cl_2 , THF, CHCl_3 , MeOH, PhH, PhCH_3 , EtOAc, and 1,4-dioxane.

It was desirable to have a “one-pot” complexation/chelation sequence to afford chelated complexes directly from benzimidazolium salt **21**. This was accomplished by simply adding exogenous base during the metalation procedure. Thus, treatment of benzimidazolium salt **21** with Pd(OAc)_2 and NaOAc provided the chelated complex **23·Pd** in 91% yield. Reactions were routinely conducted in DMSO or THF; however other polar

(48) (a) Zou, G.; Huang, W.; Xiao, Y.; Tang, J. *New J. Chem.* **2006**, *30*, 803. (b) Huynh, H. V.; Neo, T. C.; Tan, G. K. *Organometallics* **2006**, *12*, 1298. (c) Page, P. C. B.; Buckley, B. R.; Christie, S. D. R.; Edgar, M.; Poulton, A. M.; Elsegood, M. R. J.; McKee, V. J. *Organomet. Chem.* **2005**, *690*, 6210. (d) Huynh, H. V.; Ho, J. H. H.; Neo, T. C.; Koh, L. L. J. *Organomet. Chem.* **2005**, *690*, 3854. (e) Hahn, F. E.; von Fehren, T.; Lügger, T. *Inorg. Chim. Acta* **2005**, *358*, 4137. (f) Marshall, C.; Ward, M. F.; Harrison, W. T. A. *Tetrahedron Lett.* **2004**, *45*, 5703. (g) Hahn, F. E.; Holtgrewe, C.; Pape, T. Z. *Naturforsch.* **2004**, *59b*, 1051. (h) Hahn, F. E.; von Fehren, T.; Wittenbecher, L.; Fröhlich, R. Z. *Naturforsch.* **2004**, *59b*, 541. (i) Baker, M. V.; Skelton, B. W.; White, A. H.; Williams, C. C. J. *Chem. Soc., Dalton Trans.* **2001**, 111. (j) Hahn, F. E.; Foth, M. J. *Organomet. Chem.* **1999**, *585*, 241.

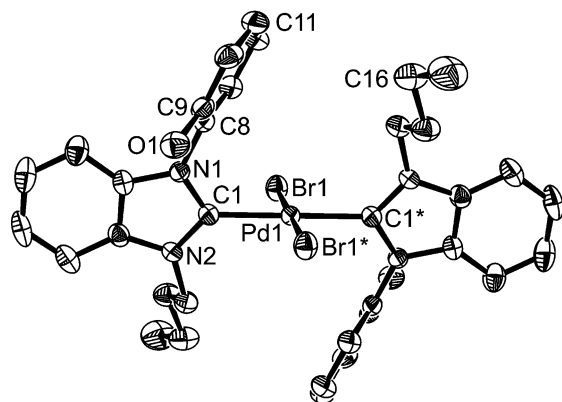
(49) Two crystallographically unique molecules were found in the unit cell. However, they were found to be superficially identical, and for clarity, only one is represented in the figures and discussed in the text.

(50) The ^1H NMR spectrum of crystals of **23·Pd** (confirmed by X-ray to be a cis complex) matched that of the crude powder.

(47) Alkylations were also successful with other 1° alkyl halides; the application of these and related ligands will be discussed in due course.

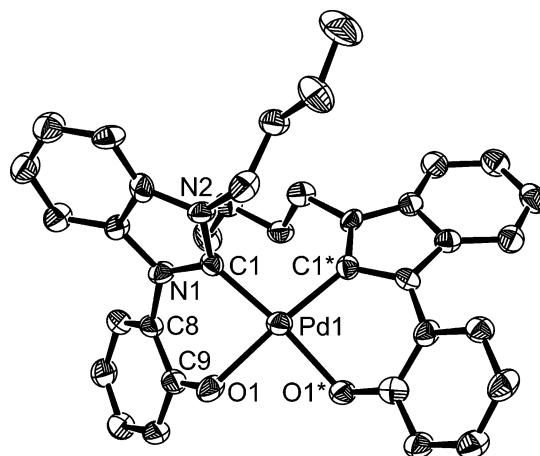
Table 1. Selected Bond Lengths, Angles, and Crystal Data for **22·Pd** and **23**

	22·Pd·2DMSO	23·Pd·H₂O	23·Ni	23·Pt·H₂O	
		Bond Lengths (Å)			
M–C1	2.024(3)	1.937(6)	1.839(2)	1.941(11)	
N1–C1	1.353(4)	1.372(7)	1.367(2)	1.376(16)	
M–X (O, Br, Cl)	2.4461(4)	2.044(4)	1.895(5)	2.040(8)	
		Angles (deg)			
N1–C1–N2	106.7(3)	105.6(5)	106.2(7)	106.6(9)	
C1–M–C1*	180.00(18)	99.3(3)	94.5(3)	100.9(5)	
C1–M–O1		86.5(2)	88.3(9)	86.7(4)	
C1–M–O1*		173.2(2)	168.9(6)	171.9(4)	
C1–N1–C8–C9	110.3(4)	–34.4(8)	26.7(3)	–33.6(18)	
		Crystal Data			
empirical formula	C ₃₄ H ₃₆ Br ₂ N ₄ O ₂ Pd·2(CH ₃) ₂ SO	C ₃₄ H ₃₄ N ₄ O ₂ Pd·H ₂ O	C ₃₄ H ₃₄ N ₄ NiO ₂	C ₃₄ H ₃₄ N ₄ O ₂ Pt·H ₂ O	
fw	955.14	655.07	589.36	743.76	
cryst syst	monoclinic	triclinic	monoclinic	triclinic	
space group	<i>P</i> 2 ₁ / <i>c</i>	<i>P</i> $\bar{1}$	<i>P</i> 2 ₁ / <i>n</i>	<i>P</i> $\bar{1}$	
<i>a</i> , Å	9.5039(3)	12.4990(4)	12.8694(2)	12.5210(5)	
<i>b</i> , Å	10.6594(4)	13.8210(5)	10.3815(2)	13.8700(6)	
<i>c</i> , Å	20.8233(9)	18.5590(7)	21.7249(4)	18.6940(10)	
α , deg	90	90.2940(15)	90	90.248(2)	
β , deg	101.660(2)	102.5920(14)	96.904(1)	102.670(2)	
γ , deg	90	99.4230(14)	90	99.0040(17)	
<i>V</i> , Å ³	2065.99(14)	3083.93(19)	2881.48(9)	3125.9(2)	
<i>T</i> , K	153(2)	153(2)	233(2)	153(2)	
<i>Z</i>	2	4	4	4	
<i>D</i> _{calc} , Mg/m ³	1.535	1.411	1.359	1.580	
cryst size (mm)	0.22 × 0.21 × 0.17	0.20 × 0.06 × 0.05	0.20 × 0.16 × 0.12	0.14 × 0.13 × 0.05	
no. of reflns collected	7923	12 704	13 775	11 823	
no. of indep reflns	4689	12 706	13 779	6579	
<i>R</i> ₁ , w <i>R</i> ₂ [<i>I</i> > 2σ(<i>I</i>)]	0.0401, 0.0894	0.0683, 0.1011	0.0407, 0.0891	0.0654, 0.1355	
goodness of fit	1.054	1.140	1.017	1.018	

**Figure 5.** ORTEP diagram of the molecular structure of **22·Pd**. Selected bond lengths, angles, and crystal data are summarized in Table 1. Ellipsoids are drawn at the 50% probability level. Hydrogen atoms and solvent molecules have been removed for clarity.

organic solvents (EtOH, CH₃CN, etc.) were also found to facilitate efficient complexation.⁵¹ The effects of chelation on thermal stability were probed using TGA. Complex **22·Pd** exhibited a *T*_d = 287 °C, whereas complex **23·Pd** exhibited a *T*_d = 311 °C (both under nitrogen) (Figure 7). The 24 °C increase in decomposition temperature is believed to be predominately due to chelation effects.⁵²

Having confirmed chelation, and enhanced thermal stability as a result of these extra intramolecular interactions, we investigated the susceptibility of other transition metals to undergo chelation to provide stable complexes. In particular, incorporation of Ni(II) would expand the relatively narrow scope

**Figure 6.** ORTEP diagram of the molecular structure of **23·Pd**. Selected bond lengths, angles, and crystal data are summarized in Table 1. Ellipsoids are drawn at the 50% probability level. Hydrogen atoms and solvent molecules have been removed for clarity.⁴⁹

of synthetic methodologies for accessing benzimidazolylidene–Ni(II) complexes.³⁸ Thus, in analogy with the synthesis of **23·Pd**, benzimidazolium salt **21** was reacted with 0.5 equiv of Ni(OAc)₂·4H₂O in the presence of NaOAc in DMSO at 80 °C. Gratifyingly, this provided the corresponding Ni complex **23·Ni** in excellent yield (95%). Attempts to isolate a ligated, non-chelated Ni complex in analogy with **22·Pd** were met with limited success, which can likely be ascribed to a more favorable cyclization geometry and/or relative greater oxophilicity of Ni.

NMR, IR, and mass spectral analyses of **23·Ni** supported formation of a chelated 2:1 ligand/metal complex. The ¹³C NMR was unremarkable and displayed a single carbene resonance at δ = 173 ppm, which was intermediate with known benzimidazolylidene (~184 ppm)³⁸ and imidazolylidene (~164–170

(51) Reactions conducted in PhCH₃, PhH, and CH₂Cl₂ were unsuccessful and resulted in incomplete consumption of starting materials ascribed to the poor solubility of the azolium, metal, and/or NaOAc salts.

(52) Although chelation is a dominant contributor, the lack of halogen ligands at the metal center may also partially explain the relatively enhanced thermal stabilities.

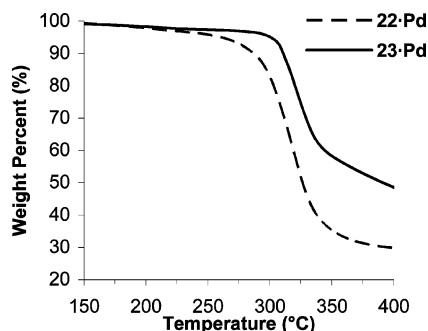


Figure 7. TGA data for complexes **22·Pd** (---) and **23·Pd** (—) taken under nitrogen atmosphere; heating rate = 10 °C/min.

ppm)^{29e,53} Ni(II) complexes. Interestingly, and in contrast to **23·Pd**, the butyl groups in **23·Ni** showed diastereotopic signals in the ¹H NMR spectrum, with some signals appearing markedly upfield in comparison with other NHC–Ni complexes.^{29,37,38} In particular, NCH₂ resonances typically appear between δ = 4.5 and 6.5 ppm, depending on the nature of the alkyl groups. In **23·Ni** however, the diastereotopic protons associated with the NCH₂ fragment appeared at δ = 4.2 and 3.6 ppm. One plausible explanation for the observed diastereotopicity in the ¹H NMR spectrum can be drawn from the X-ray data (see below), which revealed a π -facial interaction between each butyl group and the benzimidazolylidene moiety of its complementary ligand. Although this arrangement is superficially similar to that of **23·Pd**, the distances between the methylene units and the complementary benzimidazolylidene moiety in **23·Ni** are shorter than in the Pd analogue. For example, the interatomic distance between the NCH₂ carbon and the nearest atom of the complementary benzimidazolylidene moiety (i.e., C1) in **23·Ni** is 3.20 Å. The same interatomic measurement in **23·Pd** is 3.54 Å.

Quality crystals suitable for X-ray diffraction analysis were obtained as yellow plates by slow diffusion of hexanes into a saturated THF solution of **23·Ni**. As shown in the ORTEP diagram in Figure 8, the molecular structure of **23·Ni** revealed that the complex adopted a cis geometry about the metal center, which to the best of our knowledge is the first Ni complex comprised of two benzimidazolylidenes of this relative configuration. The metal center displayed a distorted square-planar arrangement with C1–Ni–C1*, C1–Ni–O1 (cis), and O1–Ni–O1* bond angles of 94.5°, 89.0°, and 90.5°, respectively. Analogous to the Pd complex, the Ni–C_{carbene} bond lengths were shortened (1.84 Å) relative to known bis(benzimidazolylidene)–Ni(II) halide complexes (1.89–1.91 Å),³⁸ again likely due to chelation in conjunction with trans influences. The N–C–N bond angles of complex **23·Ni** (106.2°) were as expected for azolylidene–Ni(II) complexes.^{37,38}

The thermal stability of **23·Ni** was investigated using TGA which revealed a T_d = 286 °C (under nitrogen); a result that reiterated the positive effects of chelation in these types of NHC complexes. Similar to the Pd complex **23·Pd**, **23·Ni** was found to be stable toward air and moisture (in solution and in the solid-state). Both complexes could be purified chromatographically on neutral alumina and, as expected, exhibited similar solubilities in common organic solvents.

To complete the series of group 10 model systems, we targeted Pt-based complex **23·Pt** (Scheme 2). Chelation to form

23·Pt required additional reaction periods at elevated temperatures, relative to its Ni and Pd analogues, which may be ascribed to the reduced oxophilicity of Pt. More specifically, whereas chelation from **22·Pd** could be completed within 1 h using Na₂CO₃ at room temperature, complete formation of **23·Pt** (monitored by ¹H NMR spectroscopy) in the presence of Na₂CO₃ in DMSO required 8 h at 80 °C (up to 24 h when NaOAc was used in lieu of Na₂CO₃).⁵⁴ Upon completion, the desired Pt complex was isolated as a single isomer in 93% yield. Full chelation was confirmed through IR and NMR spectroscopy, as well as mass spectral analysis, and solubilities resembled those of the Ni and Pd analogues. Although the solid-state structure (see below) was isostructural with **23·Pd**, the ¹H NMR spectrum more closely resembled the Ni analogue with regard to chemical shifts and splitting patterns for the butyl groups. Specifically, diastereotopic NCH₂ resonances appeared at δ = 4.0 and 3.8 ppm in the ¹H NMR spectrum of **23·Pt**. The ¹³C NMR spectrum of this same complex showed resonances at δ = 161 and 158 ppm, either of which could reasonably be assigned to the carbene atom.⁵⁵ Considering that there are very few benzimidazolylidene–Pt(II) complexes known^{6b,56} and that the range of NCN ¹³C NMR resonances of known imidazolylidene– and imidazolylidene–Pt(II) complexes varies from 143–191 ppm,⁵⁷ full assignment of the ¹³C signals from **23·Pt** cannot be made at this time.

To confirm and study the structure of **23·Pt**, X-ray quality crystals were obtained as colorless plates by slow evaporation of a THF solution of the complex. An ORTEP diagram of the molecular structure of **23·Pt** is shown in Figure 9.⁴⁹ Although the N–C–N bond angle (106.7°) was consistent with other Pt(II)-based azolylidene complexes, the Pt–C_{carbene} bond length (1.94 Å) was shorter than typically observed (1.96–2.04 Å).^{6b,56–58} Similar to chelated complexes **23·Pd** and **23·Ni**, the Pt analogue exhibited an enhanced T_d of 314 °C by TGA and could be purified by column chromatography on neutral alumina.

Overall, the model systems provide a comprehensive view of chelation effects in group 10 metals, and key characterization data are summarized in Table 2. Chelation from the phenol moieties was qualitatively observed to be progressively slower from Ni to Pd to Pt, a reflection of their relative oxophilicities. The respective metal–C_{carbene} bond lengths were generally shorter in complexes **23** when compared to known azolylidene complexes with the same metal(II) species. Chelation resulted in a change in the geometry of the metal center from trans (**22·Pd**) to cis (**23·Pd**), as well as increased thermal stability as determined using TGA. Interestingly, the cis configuration observed for each model system resulted in C₂-symmetric planar

(54) The non-chelated Pt intermediate analogous to **22·Pd** was observed by NMR spectroscopy (diagnostic signals: phenol ¹H at approximately δ = 10.0 ppm and absence of azolium ¹H at δ = 10.8 ppm).

(55) As with **23·Pd** and **23·Ni**, the oxygen-substituted carbon of the phenol ring also appears in this range and is also consistent with one of the two signals observed in **23·Pt**.

(56) Demidov, V. N.; Kukushkin, Y. N.; Vedeneeva, L. N.; Belyaev, A. N. *Zh. Obshch. Khim.* **1988**, *58*, 738.

(57) (a) Bacciu, B.; Cavell, K. J.; Fallis, I. A.; Ooi, L. *Angew. Chem., Int. Ed.* **2005**, *44*, 5282. (b) Frøseth, M.; Netland, K. A.; Rømming, C.; Tilset, M. *J. Organomet. Chem.* **2005**, *690*, 6125. (c) Liu, Q.-X.; Xu, F.-B.; Li, Q.-S.; Song, H.-B.; Zhang, Z.-Z. *J. Mol. Struct.* **2004**, *697*, 131. (d) Liu, Q.-X.; Xu, F.-B.; Li, Q.-S.; Song, H.-B.; Zhang, Z.-Z. *Organometallics* **2004**, *23*, 610. (e) Quezada, C. A.; Garrison, J. C.; Tessier, C. A.; Youngs, W. J. *J. Organomet. Chem.* **2003**, *671*, 183. (f) Meuhlhofer, M.; Strassner, T.; Herdtweck, E.; Herrmann, W. A. *J. Organomet. Chem.* **2002**, *660*, 121. (g) Hasan, M.; Kozhevnikov, I. V.; Siddiqui, R. H.; Femoni, C.; Steiner, A.; Winterton, N. *Inorg. Chem.* **2001**, *40*, 795.

(58) (a) Poyatos, M.; Maisse-François, A.; Bellemin-Lapponnaz, S.; Gade, L. H. *Organometallics* **2006**, *25*, 2634. (b) Liu, Q.-X.; Song, H.-B.; Xu, F.-B.; Li, Q.-S.; Zeng, X.-S.; Leng, X.-B.; Zhang, Z.-Z. *Polyhedron* **2003**, *22*, 1515.

(53) (a) Chamizo, J. A.; Morgado, J. *Transition Met. Chem.* **2000**, *25*, 161. (b) Herrmann, W. A.; Schwarz, J.; Gardiner, M. G.; Spiegler, M. *J. Organomet. Chem.* **1999**, *18*, 4584. (c) Lappert, M. F.; Pye, P. L. *J. Chem. Soc., Dalton Trans.* **1977**, 2172.

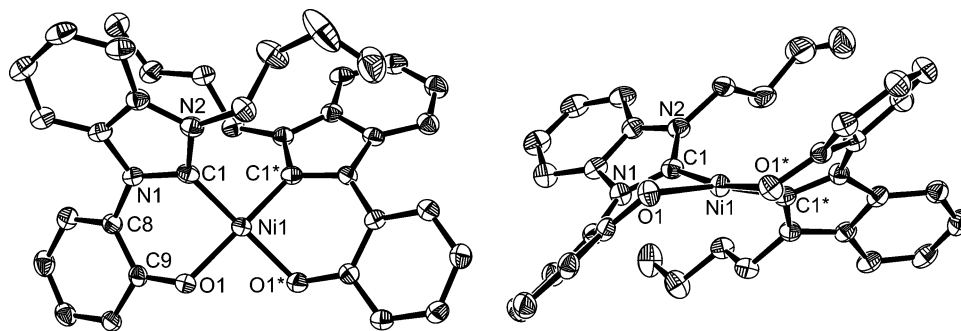


Figure 8. ORTEP diagrams of the molecular structure of **23·Ni**. Selected bond lengths, angles, and crystal data are summarized in Table 1. Ellipsoids are drawn at the 50% probability level. Hydrogen atoms have been removed for clarity.

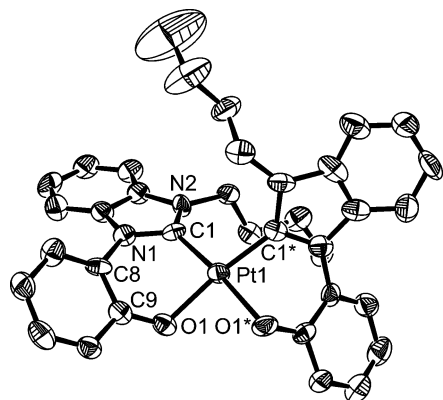


Figure 9. ORTEP diagram of the molecular structure of **23·Pt**. Selected bond lengths, angles, and crystal data are summarized in Table 1. Ellipsoids are drawn at the 50% probability level. Hydrogen atoms and solvent molecules have been removed for clarity.⁴⁹

Table 2. Key Characterization Data for Complexes **22·Pd and **23****

complex	yield (%) ^a	<i>T</i> _d (°C) ^b	λ_{max} (nm) ^c	δ NCN (ppm)
22·Pd	93	287	284	181
23·Pd	91	311	285	178
23·Ni	95	286	319	173
23·Pt	93	314	290, 343 (sh)	161 or 158 ^d

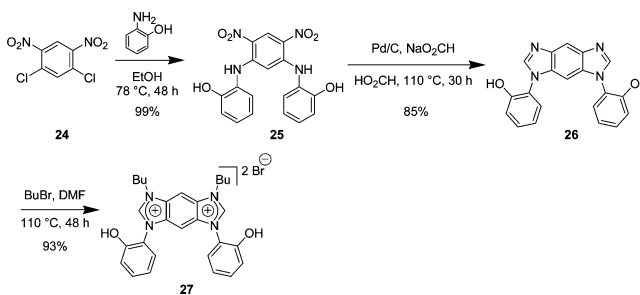
^a Isolated yields based on **21**. ^b The decomposition temperature (*T*_d) is defined as the temperature at which 10% weight loss occurs, as determined by thermogravimetric analysis under N₂ with a rate = 10 °C/min. ^c Determined in DMF under ambient conditions. ^d See discussion in the text.

chiral complexes. Although the crystals formed as racemates, separation of these enantiomers may ultimately open new avenues to optically active metal species with potential application in asymmetric catalysis.

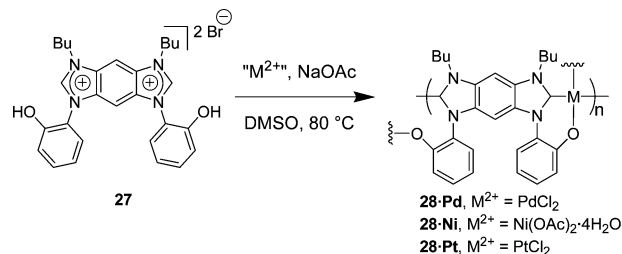
Having confirmed chelation and proof of structure in each of the group 10 model complexes, we turned our attention toward synthesizing main-chain organometallic polymers containing chelating benzimidazolylidenes. Considering that benzobis(imidazolylidene)s have a high propensity to form metal adducts at each carbene moiety of the ditopic ligand,¹⁵ installation of a single chelating N-substituent on each imidazole moiety should provide a monomer capable of forming chelated metal centers at each terminus.

As shown in Scheme 4, the corresponding ditopic bis-(bidentate) benzobis(imidazolium) monomer was synthesized by the same general reaction sequence that was used for the synthesis of **21**: S_NAr, reductive cyclization, and alkylation. In particular, treatment of readily available 1,5-dichloro-2,4-dinitrobenzene **24** with 2-aminophenol (4.0 equiv) in refluxing EtOH provided 1,5-bis[(2-hydroxyphenyl)amino]-2,4-dinitroben-

Scheme 4. Synthesis of Bis(phenolic) Benzobis(imidazolium) Monomer **27**



Scheme 5. Copolymerization with Various Transition Metals To Form Organometallic Polymers **28**



zene (**25**) in nearly quantitative yield. The in situ reductive cyclization protocol described above was successfully applied to **25** and provided benzobis(imidazole) **26** in 85% yield. Finally, alkylation with 1-bromobutane provided bis(azolium) dibromide **27** in 93% yield (78% overall yield from **24**).⁴⁷

As shown in Scheme 5, polymerizations were conducted using the conditions optimized for the synthesis of model complexes **23**. Combining a stoichiometric amount of metal salt⁵⁹ with **27** and NaOAc⁶⁰ in DMSO at 80 °C gave polymers **28·Pd**, **28·Ni**, and **28·Pt** in 99, 96, and 95% yields, respectively.⁶¹ The Pd- and Pt-based systems **28·Pd** and **28·Pt** were tan powders, whereas the Ni-based polymer **28·Ni** was a dark brown powder. Each of the polymers noted above were characterized by IR spectroscopy, NMR spectroscopy, gel permeation chromatography (GPC), UV-vis spectroscopy, and TGA; key information is summarized in Table 3.

The availability of non-chelated complex **22·Pd** allowed for direct comparison of IR spectra obtained for the corresponding

(59) Pd(OAc)₂ was found to be equally as effective as PdCl₂.

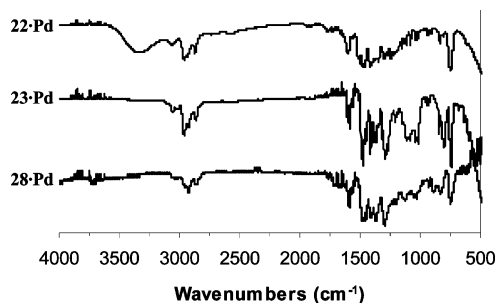
(60) A 4:1 ratio of total acetate ions relative to bis(azolium) salt **27** was used.

(61) The reactions were monitored as follows: Stirring was stopped and solids were allowed to settle. An aliquot was taken and analyzed by No-D ¹H NMR spectroscopy for the consumption of azolium starting material. For a reference describing No-D NMR technique, see: Hoye, T. R.; Eklov, B. M.; Ryba, T. D.; Voloshin, M.; Yao, L. *J. Org. Lett.* **2004**, *6*, 953.

Table 3. Physical Characterization and Absorption Maxima of Polymers 28

metal	yield (%) ^a	M_n (kDa) ^b	M_w/M_n	T_d (°C) ^c	λ_{\max} (nm) ^d
Pd	99	67.5	2.20	342	312
Ni	96	7.68 ^e	1.09 ^e	362	322
Pt	95	363	1.59	340	316, 372 (sh)

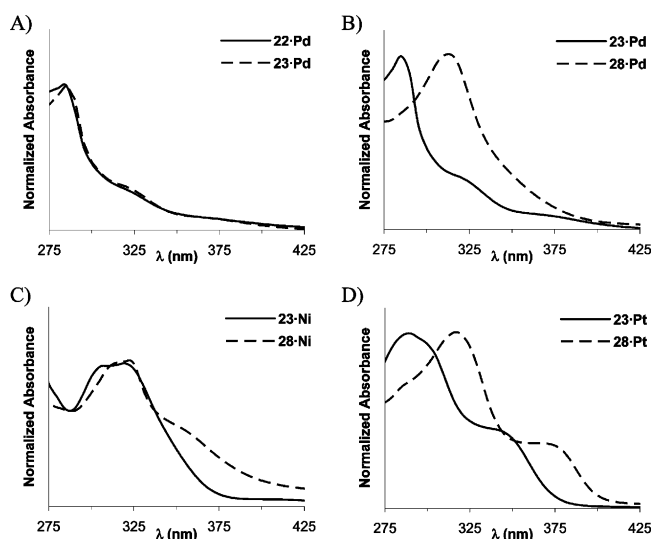
^a Isolated yields. ^b Determined by GPC relative to polystyrene standards in DMF with 0.01 M LiBr at 40 °C. ^c The decomposition temperature (T_d) is defined as the temperature at which 10% weight loss occurs, as determined by thermogravimetric analysis under N₂ with a rate = 10 °C/min. ^d Determined in DMF under ambient conditions. ^e Poor solubility of **28·Ni** resulted in fractionation.

**Figure 10.** IR spectra of (top to bottom) **22·Pd**, **23·Pd**, and **28·Pd**.

chelated monomer (**23·Pd**) and its respective polymer (**28·Pd**) (Figure 10). It was clear that the signal corresponding to the OH stretching frequency at approximately 3330 cm⁻¹ was absent in both (small molecule and polymeric) chelated systems. Similar spectra were observed for polymers **28·Ni** and **28·Pt**, which also supported chelated structures. This was further supported by ¹H NMR spectroscopy, as polymers **28** did not show any signals indicative of free phenol hydroxyl groups (e.g., $\delta \sim 10$ ppm in DMSO-*d*₆). In general, the ¹H NMR spectra of the polymers **28** were broadened and shifted upfield relative to their respective monomer **27**. The ¹H NMR signals corresponding to the butyl groups in **28** were suggestive of diastereotopic signals for each of the metals used. Specifically, the NCH₂ signals were broad multiplets appearing between 4.1 and 5.0 ppm. Considering the NMR data in combination with the rapid and exclusive formation of cis isomers in the model systems (**23**), the metal centers in **28** are assumed to be of high cis content.

Polymer **28·Ni** was only slightly soluble in common polar solvents (e.g., DMSO, DMF, and NMP), which manifested in low molecular weight material as determined by GPC ($M_n = 7,680$ g/mol, relative to polystyrene standards). The polydispersity of this polymer was also extraordinarily narrow (PDI = 1.09), which was believed to be due to selective fractionation of insoluble high molecular weight material. In contrast, the Pd- and Pt-based polymers **28** were highly soluble in polar solvents and afforded polymers with M_n s of 67,500 and 363,000 g/mol, respectively. The polydispersity indices (PDIs) of these materials were 1.6 and 2.2, respectively, and typical of step-growth polymerizations. Qualitatively, each of the polymers (**28·Pd**, **28·Ni**, and **28·Pt**) were found to be stable toward water and oxygen, as no signs of degradation (as determined by ¹H NMR spectroscopy and GPC analysis) were observed upon prolonged standing in wet, aerated solvents. Quantitative TGA of polymers **28** indicated that their T_d s ranged from 340 to 362 °C. This represented a 50–80 °C increase in thermal stability in comparison with their analogous organometallic polymers containing (non-chelating) N-alkyl substituents.^{24,52}

After model metal complexes **23** and their respective polymers **28** were synthesized, it was possible to independently study

**Figure 11.** Electronic absorption spectra of metal complexes and related polymers in DMF at room temperature.

and compare the electronic effects resulting from chelation as well as polymerization using UV-vis spectroscopy (Figure 11). The effects of chelation on the overall electronic properties were investigated by comparing non-chelated **22·Pd** with chelated analogue **23·Pd** (Figure 11A). The two spectra nearly overlap, which suggested that chelation had minimal impact on the electronic characteristics of the chromophore. Ultimately, this may provide a general means to adjust physical characteristics of NHC-based metal complexes without compromising control over their electronic properties. Additional support was obtained after analyzing polymers **28·Pd** ($\lambda_{\max} = 312$ nm) and **28·Pt** ($\lambda_{\max} = 316$ nm); these polymers exhibit λ_{\max} values in the same range as similar Pd- and Pt-based polymers that do not contain chelating N-substituents (λ_{\max} values ranged from 314–329 nm).²⁴

To determine if delocalization occurred along the main-chain of polymers **28**, we compared each model complex with its corresponding polymer (Figure 11B,C). In general, the λ_{\max} values of the polymers were bathochromically shifted from their respective model complexes. In particular, Pd- and Pt-based polymers (**28·Pd** and **28·Pt**) were red-shifted 27 and 26 nm when compared to **23·Pd** (Figure 11B) and **23·Pt** (Figure 11C), respectively. In contrast, polymer **28·Ni** was red-shifted by only 3 nm relative to model complex **23·Ni**, which may be partially explained by fractionation and detection of only low molecular weight material (see above). The Ni polymer does, however, show increased relative absorption intensities at longer wavelengths (>335 nm) in comparison with the model system. The electronic fine structures of polymers **28** were also in good agreement with those of model complexes **23**, as concluded by comparing the topologies of the corresponding spectra. For example, vibronic contributions in the Ni-based systems were manifested in two distinguishable local maxima (Figure 11C) between 300 and 325 nm.

The general order of absorption maxima for both the models and polymers was found to be Ni > Pt ~ Pd. The increased electronic communication between the NHC moiety and the Ni(II) center may be due to the lower electronegativity of Ni in combination with better orbital overlap between the NHC and the smaller Ni center (relative to Pd and Pt). In both the models and the polymers, the Pd- and Pt-based compounds showed similar absorption maxima. This is as would be expected given their nearly identical electronegativities and the observation that **23·Pd** and **23·Pt** were isostructural in the solid-state. Overall,

the electronic absorption data were encouraging because they supported the possibility of the main-chain polymers **28** exhibiting long-range, through-metal electronic communication.

Conclusion

In summary, we describe the synthesis and characterization of a series of group 10 metal–carbene complexes and organometallic polymers comprised of a new chelating benzimidazolylidene. The model complexes were prepared in 91–95% yields via direct metalation of a N-(*o*-phenol)-substituted benzimidazolium bromide using Pd(II), Ni(II), or Pt(II) salts. The synthesis of the requisite benzimidazolium salt was completed in three steps in 85% yield from commercial material. This synthesis was borne out through the development of a one-pot reduction/cyclization protocol which converted *o*-nitroanilines to benzimidazoles in high yields. A modular feature of this ligand design is that the final N-substituent (i.e., the butyl group) may be varied to control physical characteristics such as solubility and processability.⁴⁷

A ligated but non-chelated Pd(II) complex (**22·Pd**) was also obtained that allowed for direct comparison of the effects of chelation on bonding geometry, thermal stability, and electronic characteristics. Interestingly, it was observed that the non-chelated trans Pd complex was converted into the corresponding cis isomer upon chelation, a geometry that was observed for each of the chelated complexes. In addition, chelation provided increased thermal stability, which was manifested in a 24 °C increase in T_d on going from **22·Pd** to **23·Pd**. The structures of the model complexes were supported by NMR and IR spectroscopy and unambiguously confirmed through X-ray crystallographic analysis. The ¹H NMR spectra of the Ni- and Pt-based complexes displayed diastereotopic butyl groups, whereas the Pd complex exhibited no diastereotopicity. Each of the model complexes contained shorter metal–C_{carbene} bonds than generally observed for NHC complexes of the same metal species.

These results formed the basis for the design of a new class of organometallic polymers. An annulated benzobis(imidazolium) salt bearing N-(*o*-phenol) substituents was synthesized by a short S_NAr–reduction/cyclization–alkylation sequence in 78% overall yield without the need for chromatography. Direct metalation with Pd(II), Ni(II), or Pt(II) salts afforded the respective main-chain organometallic polymers in 95–99% isolated yields. The resulting organometallic polymers contained a benzobis(imidazolylidene) with pendent N-(*o*-phenol) groups that were found to coordinate to transition metals in a chelating-type fashion, as confirmed by ¹H NMR and IR spectroscopies. This resulted in polymeric materials with molecular weights up to 363,000 g/mol (relative to polystyrene standards) and PDIs typical of step-growth polymerizations. The polymers showed excellent moisture- and air-stability in both solution and solid-state. TGA analysis of the polymers revealed that T_{d5} ranged from 340 to 362 °C (under nitrogen), which correspond to a 50–80 °C increase in thermal stability relative to previously reported²⁴ polymers of similar composition.

The electronic absorption spectra of the model complexes and their corresponding polymeric materials revealed several promising features. First, chelation has a minimal overall impact on the electronic characteristics of the complexes and polymers. This was confirmed through the comparison of **22·Pd** and **23·Pd**, which displayed nearly overlapping electronic absorption spectra. The λ_{max} values for the model complexes and polymers ranged from 285 to 319 nm and 312–322 nm, respectively, depending on the incorporated metal. In each series, λ_{max} increased in the order Ni > Pt ~ Pd. The polymers each

displayed electronic absorption spectra consistent in shape with the corresponding model complexes. The electronic absorption spectra of the polymers were also bathochromically shifted by 3–27 nm relative to their respective model systems, which suggested an increased delocalization character in the former. Collectively, the data indicated that the thermal stabilities of our previously reported materials were increased without a compromise in their electronic characteristics.

This new series of main-chain NHC-based polymers builds upon our recently reported procedure for preparing analogous polymers by extending the range of transition metals that may be incorporated into the main chains. Importantly, a novel ligand design facilitated the synthesis and characterization of new group 10 system, ultimately revealing that the greatest degree of electronic communication may in fact be in the Ni-based small and macromolecular complexes. Future efforts will focus on exploring the utility of these materials in catalysis and further examining their physical characteristics with an emphasis on their utilities in electronic applications

Experimental Section

Materials and Methods. ¹H and ¹³C NMR spectra were recorded using a Varian Unity Plus 300 or 400 spectrometer and were routinely run using broadband decoupling. Chemical shifts (δ) are expressed in ppm downfield from tetramethylsilane using the residual protonated solvent as an internal standard (DMSO-*d*₆, ¹H: 2.49 ppm and ¹³C: 39.5 ppm; CDCl₃, ¹H: 7.26 ppm and ¹³C: 77.0 ppm). Coupling constants are expressed in hertz (Hz). HRMS (CI) were obtained with a VG analytical ZAB2-E instrument. UV–vis spectra were recorded using a Perkin-Elmer Instruments Lambda 35 spectrometer. Infrared spectra were recorded on a Thermo IR200. GPC data was obtained using a Waters HPLC system consisting of HR-1, HR-3, and HR-5E Styragel columns arranged in series, a 1515 pump, and a 2414 RI detector. Molecular weight data are reported relative to polystyrene standards in DMF (0.01 M LiBr) at 40 °C (column temperature). Decomposition temperatures (T_{d5}) were determined using a TA Instruments TGA-Q500 under nitrogen atmosphere and were defined as the temperature at which 10% mass loss occurred. All solvents and reagents were of reagent quality and used as obtained from commercial sources. Chromatography was performed with neutral alumina (Brockmann I, 60–325 mesh).

2-(2-Nitrophenylamino)phenol (19). 1-Fluoro-2-nitrobenzene (**18**) (1.34 g, 9.48 mmol), 2-aminophenol (2.59 g, 23.7 mmol), NaHCO₃ (1.59 g, 18.96 mol), EtOH (10 mL), and a magnetic stirbar were combined in a 20 mL Schlenk flask. The mixture was stirred in an oil bath at 100 °C for 20 h. The cooled reaction mixture was filtered through Celite with the aid of 10 mL of CH₂Cl₂ and concentrated. The crude material was taken up in CH₂Cl₂ and filtered through a plug of silica gel (eluting with CH₂Cl₂). Concentration of the resulting red-orange filtrate provided 2.00 g (92% yield) of the desired material. Although this compound was previously reported, complete spectral data were not provided.⁴⁵ ¹H NMR (400 MHz, CDCl₃): δ 9.01 (br s, 1H), 8.21 (dd, J = 8.4, 1.6 Hz, 1H), 7.40–7.35 (m, 1H), 7.28–7.20 (m, 2H), 7.07 (dd, J = 8.0, 1.2 Hz, 1H), 6.99 (ddd, J = 7.8, 7.6, 1.2 Hz, 1H), 6.84–6.79 (m, 1H), 6.77 (dd, J = 8.6, 1.4 Hz, 1H), 5.63 (br s, 1H). ¹³C NMR (100 MHz CDCl₃): δ 152.2, 144.0, 136.1, 133.6, 128.9, 127.8, 126.5, 124.9, 121.4, 118.1, 116.3, 116.2. HRMS: m/z calcd for C₁₂H₁₁N₂O₃ [M + H⁺] 231.0770, found 231.0775.

N-(2-Hydroxyphenyl)benzimidazole (20). A 100 mL flask was charged with a magnetic stirbar, formic acid (88%, 60 mL), NaO₂-CH (1.77 g, 26.1 mmol), and 10% Pd/C (460 mg, 0.43 mmol Pd). After adding nitroarene **19** (2.00 g, 8.69 mmol) to this mixture, this flask was fitted with a H₂O-jacketed condenser and stirred in an oil bath at 110 °C for 7 h. Upon completion, the cooled reaction mixture was filtered through Celite with the aid of 25 mL of H₂O

and the volume of the filtrate was reduced to approximately 10 mL, under reduced pressure. The acidic solution was then slowly added to a vigorously stirred aqueous solution of saturated Na_2CO_3 (250 mL). The resulting solids were collected by vacuum filtration, rinsed with H_2O , and dried under vacuum to give 2.12 g (93% yield) of monosubstituted benzimidazole **20** as a tan solid. This material was routinely used without additional purification. Although this compound was previously reported, complete spectral data were not provided.⁴⁶ ^1H NMR (400 MHz, $\text{DMSO}-d_6$): δ 8.29 (s, 1H), 7.72 (br s, 1H), 7.34 (d, $J = 7.6$ Hz, 1H), 7.29–7.22 (m, 4H), 7.11 (d, $J = 8.4$ Hz, 1H), 6.89 (t, $J = 7.2$ Hz, 1H). ^{13}C NMR (100 MHz, $\text{DMSO}-d_6$): δ 152.2, 144.4, 143.0, 134.3, 129.7, 127.5, 122.9, 122.9, 121.9, 119.6, 119.5, 117.0, 111.1. HRMS: m/z calcd for $\text{C}_{13}\text{H}_{11}\text{N}_2\text{O}$ [$\text{M} + \text{H}^+$] 211.0871, found 211.0873.

***N*-Butyl-*N'*-(2-hydroxyphenyl)benzimidazolium Bromide (21).**

In a 20 mL screw-cap vial, benzimidazole **20** (347 mg, 1.65 mmol) was dissolved in a mixture of CH_3CN (5.0 mL) and 1-bromobutane (0.53 mL, 4.95 mmol). After adding a magnetic stirbar, the vial was sealed with a Teflon-lined cap, placed in an oil bath at 100 °C, and then stirred for 12 h. After cooling to ambient temperature, the reaction mixture was transferred to a round-bottom flask with the aid of 3 mL of MeOH. The crude material was then concentrated under reduced pressure to provide benzimidazolium bromide **21** as the sole detectable product in >99% yield. Recrystallization from hot $\text{CH}_2\text{Cl}_2/\text{hexanes}$ gave colorless needles. ^1H NMR (400 MHz, $\text{DMSO}-d_6$): δ 10.75 (s, 1H), 10.11 (s, 1H), 8.21 (d, $J = 8.0$ Hz, 1H), 7.76–7.69 (m, 3H), 7.58–7.51 (m, 2H), 7.22 (d, $J = 0.8$ Hz, 1H), 7.11 (ddd, $J = 8.0, 7.6, 1.2$ Hz, 1H), 4.59 (t, $J = 7.2$ Hz, 2H), 1.96 (pent, $J = 7.2$ Hz, 2H), 1.39 (sext, $J = 7.2$ Hz, 2H), 0.95 (t, $J = 7.2$ Hz, 3H). ^{13}C NMR (100 MHz, $\text{DMSO}-d_6$): δ 152.2, 143.2, 132.1, 131.7, 130.8, 127.9, 127.2, 126.7, 112.0, 119.8, 117.3, 114.0, 46.8, 30.5, 19.1, 13.4. HRMS: m/z calcd for $\text{C}_{17}\text{H}_{19}\text{N}_2\text{O}$ [M^+] 267.1497, found 267.1494.

Palladium Dibromide Complex 22·Pd. After suspending benzimidazolium bromide **21** (598 mg, 1.72 mmol) in THF (15 mL), $\text{Pd}(\text{OAc})_2$ (193 mg, 0.86 mmol) was added. The resulting mixture was then vigorously stirred at 50 °C for 2 h, allowed to cool, filtered through a thin pad of alumina, and then concentrated under vacuum to give 639 mg (93% yield) of complex **22·Pd** as a tan powder. Crystals suitable for X-ray analysis were obtained by dilution of an NMR sample (in $\text{DMSO}-d_6$) with THF (4-fold by volume) and diffusion of hexanes into this mixture. Anal. Calcd for $\text{C}_{34}\text{H}_{36}\text{N}_4\text{O}_2\text{Br}_2\text{Pd}\cdot\text{H}_2\text{O}$: C, 49.99; H, 4.54; N, 7.04. Found: C, 49.84; H, 4.43; N, 6.53. ^1H NMR (400 MHz, $\text{DMSO}-d_6$): δ 7.55–7.49 (m, 4H), 7.38 (d, $J = 8.0$ Hz, 2H), 7.33 (dd, $J = 8.2, 1.4$ Hz, 2H), 7.31–7.27 (m, 2H), 7.23–7.18 (m, 4H), 7.01–6.98 (m, 2H), 4.40–4.29 (m, 4H), 1.85–1.79 (m, 4H), 1.29–1.23 (m, 4H), 0.94 (t, $J = 7.4$ Hz, 6H). ^{13}C NMR (75 MHz $\text{DMSO}-d_6$): δ 181.2, 152.2, 136.2, 134.1, 131.1, 130.7, 126.2, 123.5, 121.9, 120.4, 111.3, 110.5, 109.7, 106.7, 48.3, 44.5, 31.4, 20.3, 14.0. IR (KBr): 3331, 3061, 2958, 2931, 2872, 1591, 1500, 1462, 1416, 1344 cm^{-1} . HRMS: m/z calcd for $\text{C}_{34}\text{H}_{36}\text{N}_4\text{O}_2\text{Br}_2\text{Pd}$ [M^+] 794.0245, found 794.0240.

Chelated Palladium Complex 23·Pd. Direct procedure: After dissolving benzimidazolium bromide **21** (200 mg, 0.58 mmol) in DMSO (10 mL), $\text{Pd}(\text{OAc})_2$ (58 mg, 0.26 mmol) and NaOAc (48 mg, 0.58 mmol) were added. The reaction mixture was then placed in an oil bath thermostated at 80 °C and stirred for 2 h, at which time NMR spectroscopy⁶¹ revealed complete consumption of **21**. The solution was then allowed to cool to ambient temperature and poured into H_2O (25 mL). The resulting precipitates were collected via vacuum filtration and dried under vacuum to give 151 mg (91% yield) of the chelated complex. Stepwise procedure: After dissolving benzimidazolium bromide **21** (200 mg, 0.58 mmol) in THF (10 mL), $\text{Pd}(\text{OAc})_2$ (58 mg, 0.26 mmol) was added. The reaction mixture was placed in an oil bath thermostated at 50 °C and stirred for 2 h. After allowing the mixture to cool to ambient temperature, Na_2CO_3 (256 mg, 2.32 mmol) and MeOH (10 mL) were added.

The resulting slurry was stirred for 1 h, poured into H_2O (25 mL), and extracted with EtOAc (3×10 mL). The organic extracts were washed with brine (50 mL), dried over Na_2SO_4 , filtered through a thin pad of alumina, and concentrated. Flash chromatography on neutral alumina (eluent = Et_2O) provided the desired complex in 88% yield as a yellow-gold powder. Crystals suitable for X-ray analysis were obtained by slow evaporation of a THF/hexanes mixture of the crude product mixture. Anal. Calcd for $\text{C}_{34}\text{H}_{34}\text{N}_4\text{O}_2\text{Pd}\cdot 0.5\text{H}_2\text{O}$: C, 63.21; H, 5.46; N, 8.55. Found: C, 63.81; H, 5.42; N, 8.74. ^1H NMR (400 MHz, CDCl_3): δ 7.89 (dd, $J = 7.4, 1.0$ Hz, 2H), 7.59 (dd, $J = 8.0, 1.6$ Hz, 2H), 7.54 (dd, $J = 7.4, 1.4$ Hz, 2H), 7.39–7.31 (m, 4H), 7.07–6.99 (m, 6H), 6.76 (ddd appearing as td, $J = 7.4, 1.8$ Hz, 2H), 4.86 (t, $J = 7.6$ Hz, 4H), 2.20–2.13 (m, 4H), 1.68–1.58 (m, 4H), 1.03 (t, $J = 7.6$ Hz, 6H). ^{13}C NMR (75 MHz CDCl_3): δ 177.7, 160.6, 135.4, 131.6, 130.6, 127.6, 123.5, 122.0, 121.5, 115.1, 112.9, 111, 46.0, 32.8, 20.4, 14.0. IR (KBr): 3057, 3022, 2960, 2929, 2860, 1585, 1473, 1288, 1115, 1084, 1018 cm^{-1} . HRMS: m/z calcd for $\text{C}_{34}\text{H}_{34}\text{N}_4\text{O}_2\text{Pd}$ [M^+] 636.1717, found 636.1721.

Nickel Complex 23·Ni. The complex was synthesized in analogy to **23·Pd** from azolium salt **21** (347 mg, 1.0 mmol), $\text{Ni}(\text{OAc})_2\cdot 4\text{H}_2\text{O}$ (124 mg, 0.50 mmol), and NaOAc (82 mg, 1.0 mmol) in DMSO (4.0 mL). Recrystallization of the crude material from $\text{CH}_2\text{Cl}_2/\text{hexanes}$ gave 280 mg (95% yield) of the desired product as a yellow solid. Alternatively, the crude material could be purified by flash chromatography on neutral alumina (eluent = Et_2O). Crystals suitable for X-ray analysis were obtained by slow diffusion of hexanes into a THF solution of the crude product mixture. Anal. Calcd for $\text{C}_{34}\text{H}_{34}\text{N}_4\text{O}_2\text{Ni}\cdot\text{H}_2\text{O}$: C, 67.23; H, 5.97; N, 9.22. Found: C, 67.23; H, 5.83; N, 9.17. ^1H NMR (400 MHz, CDCl_3): δ 7.91–7.89 (m, 2H), 7.67 (d, $J = 7.2$ Hz, 2H), 7.39 (d, $J = 8.4$ Hz, 2H), 7.30–7.29 (m, 6H), 7.17 (t, $J = 7.2$ Hz, 2H), 6.80 (t, $J = 7.4$ Hz, 2H), 4.23–4.16 (m, 2H), 3.64–3.57 (m, 2H), 2.32–2.28 (m, 2H), 1.32–1.24 (m, 4H), 1.11–1.04 (m, 2H), 0.55 (t, $J = 7.0$ Hz, 6H). ^{13}C NMR (75 MHz, CDCl_3): δ 172.5, 158.9, 135.3, 132.2, 128.2, 128.1, 123.72, 123.67, 122.4, 120.1, 113.9, 112.2, 109.9, 48.3, 32.1, 20.2, 13.3. IR (KBr): 3059, 3037, 2962, 2933, 2862, 1585, 1487, 1275, 1115, 1020 cm^{-1} . HRMS: m/z calcd for $\text{C}_{34}\text{H}_{35}\text{N}_4\text{O}_2\text{Ni}$ [$\text{M} + \text{H}^+$] 589.2113, found 589.2115.

Platinum Complex 23·Pt. The complex was synthesized in analogy to **23·Pd** from azolium salt **21** (120 mg, 0.35 mmol), PtCl_2 (41 mg, 0.16 mmol), and NaOAc (62 mg, 0.76 mmol) in DMSO (3.0 mL). Recrystallization of the crude material from $\text{CH}_2\text{Cl}_2/\text{hexanes}$ gave 108 mg (93% yield) of the desired product as a white solid. Alternatively, the crude material could be purified by flash chromatography on neutral alumina (eluent = 10% $\text{CH}_2\text{Cl}_2/\text{Et}_2\text{O}$). Crystals suitable for X-ray analysis were obtained by slow evaporation of a THF solution of the purified complex. Anal. Calcd for $\text{C}_{34}\text{H}_{34}\text{N}_4\text{O}_2\text{Pt}\cdot 0.5\text{H}_2\text{O}$: C, 55.58; H, 4.80; N, 7.63. Found: C, 55.35; H, 4.40; N, 7.20. ^1H NMR (400 MHz, CDCl_3): δ 7.93–7.91 (m, 2H), 7.59 (dd, $J = 7.6, 1.6$ Hz, 2H), 7.44 (dd, $J = 8.4, 1.2$ Hz, 2H), 7.39–7.30 (m, 6H), 7.23–7.19 (m, 2H), 6.79 (ddd appearing as td, $J = 8.0, 1.2$ Hz, 2H), 4.05–3.98 (m, 2H), 3.84–3.76 (m, 2H), 2.19–2.01 (m, 2H), 1.56–1.45 (m, 2H), 1.18–1.02 (m, 4H), 0.57 (t, $J = 7.4$ Hz, 6H). ^{13}C NMR (75 MHz, CDCl_3): δ 160.8, 157.8, 134.6, 132.2, 128.5, 128.2, 123.9, 123.8, 122.4, 121.2, 114.8, 112.8, 110.3, 48.1, 31.1, 20.0, 13.2. IR (KBr): 3061, 3030, 2964, 2933, 2874, 2862, 1585, 1489, 1473, 1294, 1113, 1038, 1020 cm^{-1} . HRMS: m/z calcd for $\text{C}_{34}\text{H}_{35}\text{N}_4\text{O}_2\text{Pt}$ [$\text{M} + \text{H}^+$] 726.2408, found 726.2402.

1,5-Bis[(2-hydroxyphenyl)amino]-2,4-dinitrobenzene (25). A 500 mL flask was charged with 1,5-dichloro-2,4-dinitrobenzene (10.0 g, 42.2 mmol), 2-aminophenol (18.4 g, 169 mmol), EtOH (250 mL), and a magnetic stir bar. The flask was equipped with a H_2O -jacketed condenser, and the mixture was heated under reflux for 48 h. The resulting red solution was allowed to cool to ambient temperature, and the volume was reduced to approximately half

its original volume under reduced pressure. The red slurry was then poured into H₂O (200 mL) and allowed to stand for 1 h. The red solids that had formed were collected by vacuum filtration, rinsed with H₂O, and dried under vacuum to give **25** (15.9 g, 99% yield). Although this material was routinely used without additional purification, recrystallization from hot MeOH/H₂O affords orange-red crystals. ¹H NMR (400 MHz, DMSO-*d*₆): δ 9.64 (br s, 2H), 9.04 (s, 1H), 7.21 (dd, *J* = 7.6, 1.2 Hz, 2H), 7.03 (t, *J* = 6.8 Hz, 2H), 6.92 (d, *J* = 7.4 Hz, 2H), 6.76 (t, *J* = 7.0 Hz, 2H), 6.30 (s, 1H). ¹³C NMR (100 MHz DMSO-*d*₆): δ 150.8, 145.6, 128.3, 127.0, 125.0, 124.7, 124.6, 119.2, 116.3, 95.5. HRMS: *m/z* calcd for C₁₈H₁₄N₄O₆ [M⁻] 382.0913, found 382.0912.

Benzobis(imidazole) 26. In an 500 mL flask, a suspension of 10% Pd/C (1.0 g, 0.94 mmol Pd) and NaO₂CH (22.6 g, 333 mmol) in formic acid (88%, 250 mL) was treated with dinitroarene **25** (10.6 g, 27.7 mmol) in several portions. The flask was then equipped with a H₂O-jacketed condenser, and the mixture was heated under reflux for 48 h. Upon completion, the mixture was allowed to cool to ambient temperature, filtered through Celite, and washed with 50 mL of H₂O. The filtrate volume was then reduced under vacuum to approximately 50 mL and then slowly added to a stirred aqueous solution saturated with Na₂CO₃. The resulting precipitate was collected by vacuum filtration, rinsed with H₂O, and dried under vacuum to give benzobis(imidazole) **26** (8.1 g, 85% yield) as a tan powder. The material was routinely used without additional purification. ¹H NMR (400 MHz, DMSO-*d*₆): δ 10.2 (br s, 2H), 8.31 (s, 2H), 8.02 (s, 1H), 7.39 (d, *J* = 7.6 Hz, 2H), 7.30 (t, *J* = 7.6 Hz, 2H), 7.08 (d, *J* = 8.4 Hz, 2H), 6.95 (t, *J* = 7.2 Hz, 2H), 6.91 (s, 1H). ¹³C NMR (75 MHz DMSO-*d*₆): δ 152.2, 145.0, 140.1, 132.3, 129.6, 127.6, 123.2, 119.7, 117.1, 108.4, 90.9. HRMS: *m/z* calcd for C₂₀H₁₄N₄O₂ [M⁻] 342.1117, found 342.1112.

Benzobis(imidazolium) Dibromide 27. A Schlenk flask was charged with DMF (100 mL), benzobis(imidazole) **26** (11.8 g, 34.5 mmol), 1-bromobutane (22.2 mL, 207 mmol), and a magnetic stirbar. After sealing the flask, the resulting slurry was stirred at 110 °C for 48 h, during which time the mixture became homogeneous for a short period of time and then heterogeneous. Subsequently, the cooled mixture was poured into PhCH₃ (200 mL), and the solids were collected by vacuum filtration, rinsed with THF, and dried under vacuum. Recrystallization from MeOH/THF mixture (1:3 v/v) gave 19.8 g (93% yield) of the bis(azolium) salt as a tan powder. ¹H NMR (400 MHz, DMSO-*d*₆): δ 10.77 (br s, 2H) 10.52 (s, 2H), 9.46 (s, 1H), 7.72 (dd, *J* = 8.0, 1.2 Hz, 2H), 7.53–7.49 (m, 3H), 7.22 (d, *J* = 8.4 Hz, 2H), 7.09 (t, *J* = 8.2 Hz, 2H), 4.80 (t, *J* = 6.8 Hz, 4H), 2.08 (pent, *J* = 7.4 Hz, 4H), 1.46 (sext, *J* = 7.4 Hz, 4H), 0.97 (t, *J* = 7.2 Hz, 6H). ¹³C NMR (75 MHz DMSO-*d*₆): δ 152.2, 147.0, 132.5, 130.9, 130.0, 128.1, 120.0,

119.7, 117.5, 100.0, 98.9, 47.6, 30.2, 19.1, 13.5. HRMS: *m/z* calcd for C₂₈H₃₁N₄O₂ [M – H⁺] 455.2447, found 455.2447.

General Polymerization Procedure. After dissolving bis(azolium) dibromide **27** (1.0 mmol, 1.0 equiv) in DMSO (5 mL), metal salt (1.0 mmol, 1.0 equiv) and NaOAc (2.0 mmol, 2.0 equiv if Ni(OAc)₂; 4.0 mmol, 4.0 equiv if PdCl₂ or PtCl₂) were then added to the reaction vessel. The resulting solution was then stirred at 80 °C for 24–48 h and monitored by ¹H NMR spectroscopy.⁶¹ Upon completion, the mixture was allowed to cool and added dropwise into H₂O (50 mL). The resulting precipitate was collected via vacuum filtration, rinsed with H₂O, and dried under vacuum.

Polymer 28•Pd. ¹H NMR (400 MHz, DMSO-*d*₆): δ 8.15 (br, 2H), 7.40–6.80 (br, 8H), 4.40–5.00 (br, 4H), 2.15 (br, 4H), 1.45 (br, 4H), 1.00 (br, 6H). IR (KBr): 3067, 2966, 2954, 2882, 1594, 1486, 1421, 1381, 1301 cm⁻¹.

Polymer 28•Ni. ¹H NMR (400 MHz, DMSO-*d*₆): δ 8.02 (br, 2H), 7.58–7.21 (br, 4H), 7.20–6.75 (br, 4H), 4.05–4.62 (br, 4H), 2.00 (br, 4H), 1.40 (br, 4H), 0.94 (br, 6H). IR (KBr): 3143, 3038, 2962, 2952, 2898, 1594, 1489, 1414, 1376, 1301 cm⁻¹.

Polymer 28•Pt. ¹H NMR (400 MHz, DMSO-*d*₆): δ 8.05 (br, 2H), 7.55–7.25 (br, 4H), 7.20–6.90 (br, 4H), 4.38–4.99 (br, 4H), 2.01 (br, 4H), 1.40 (br, 4H), 0.95 (br, 6H). IR (KBr): 3097, 3051, 2971, 2949, 2899, 2881, 1597, 1483, 1444, 1381, 1307 cm⁻¹.

Acknowledgment. We are grateful to the U.S. Army Research Office (W911NF-05-1-0430), the donors of the Petroleum Research Fund as administered by the American Chemical Society (44077-G1), the Welch Foundation (F-1621), and The University of Texas at Austin for their generous financial support. A.J.B. thanks UT-Austin for a graduate research fellowship. J.D.R. thanks the Beckman Foundation and UT-Austin for undergraduate research fellowships. O.L.D. thanks the Beckman Foundation, the Intel Corporation, and UT-Austin for undergraduate research fellowships. We would also like to thank Prof. Grant Willson and his group for allowing us to use their TGA, as well as Prof. Brent Iverson and his group for allowing us to use their UV–vis spectrometer.

Supporting Information Available: CIF files containing X-ray structural data, atomic coordinates, thermal parameters, bond distances, and bond angles for complexes **22•Pd**, **23•Ni**, **23•Pd**, and **23•Pt**. Data for these complexes have been deposited at the Cambridge Crystallographic Data Centre, Cambridge, UK as CCDC 625759 (**22•Pd**), CCDC 610294 (**23•Ni**), CCDC 625760 (**23•Pd**), and CCDC 625761 (**23•Pt**). This material is available free of charge via the Internet at <http://pubs.acs.org>.

OM060494U